Article DOI: https://doi.org/10.3201/eid3212.261208

EID cannot ensure accessibility for supplementary materials supplied by authors. Readers who have difficulty accessing supplementary content should contact the authors for assistance.

Rat Hepatitis E Virus and Seoul Hantavirus in Pet Rats, Germany

Appendix

Material and Methods

Nucleic acid preparation, reverse transcription-polymerase chain reaction and high-throughput sequencing

Liver tissue (for KS22/002 heart and lung tissue) was homogenized and nucleic acids extracted using NucleoMag® VET (Macherey-Nagel, Düren, Germany), per kit instructions, on a KingFisher Flex Purification System (Thermo Fisher Scientific, Waltham, MA, USA). RNA extracts were then screened for all hepevirus strains using a conventional one-step nested broad-spectrum (NBS) RT-PCR (HEV-cs 5′ – TCG CGC ATC ACM TTY TTC CAR AA – 3′ and HEV-cas 5′ – GCC ATG TTC CAG ACD GTR TTC CA – 3′; HEV-csn 5′ – TGT GCT CTG TTT GGC CCN TGG TTY CG – 3′ and HEV-casn 5′ – CCA GGC TCA CCR GAR TGY TTC TTC CA – 3′) using SuperScript III RT-PCR Kit (Qiagen, Hilden, Germany), as previously described (*1*). The NBS RT-PCR has been developed to detect a wide range of different hepeviruses (*2*). It has been shown to be capable of sensitive detection of different genotypes of hepatitis E virus (HEV, *Paslahepevirus balayani*), i.e., HEV-1, HEV-2, HEV-3 and HEV-4 (*3*) as well as a wide range of ratHEV strains (*1*,*4*). Samples were subsequently screened for rat hepatitis E virus (ratHEV; *Rocahepevirus ratti*) by real-time RT-PCR (RT-qPCR; rHEV-F 5′ – TAC CCG ATG CCG GGC AGT – 3′, rHEV-R2 5′ – ATC YAC ATC WGG GAC AGG – 3′, and rHEV-P2 5′ – FAM- AAT GAC AGC ACA GGC ACC GGC GCC-BHQ – 3′) using QuantiTect Probe RT-PCR Kit (Qiagen, Hilden, Germany), as previously described (*5*).

The RT-PCR screening of wild brown rats (*Rattus norvegicus*) from Rotterdam and Amsterdam, the Netherlands, has been described before within a study on multiple pathogens (*6*). Short open reading frame (ORF) 1 sequences from positive samples of the pet rats of this study and 12 ratHEV-RNA positive wild brown rats from the Netherlands were obtained by dideoxy chain termination sequencing performed using BigDye Terminator v1.1 Cycle Sequencing Kit (Thermo Fisher Scientific), according to the manufacturer's protocol. The partial ORF1 sequences were uploaded to GenBank with accession numbers PZ583560-PZ583571.

High-throughput sequencing (HTS), combined with a RT-PCR based sequencing of the hypervariable region (HVR; see below) was used to determine the entire ratHEV coding sequences of all three pet rat strains and three wild rat-derived strains from Rotterdam, the Netherlands, from liver tissue RNA. The latter three strains were selected out of 12 ratHEV sequences from the Netherlands (8 from Rotterdam, 4 from Amsterdam): strain M226 from Rotterdam was selected due to the high sequence similarity of the partial ORF1 sequence to the pet rat-derived sequences; two other strains (M186 and M268) were added as further strains from Rotterdam (main article Figure, panel A). Libraries were first generated using KAPA RNA HyperPrep Kit for Illumina® platforms (Roche Diagnostics, Mannheim, Germany), followed by enrichment of HEV nucleic acids (excluding the HVR) using HEV-specific myBaits® (Arbor Bioscience, Ann Arbor, MI, USA), as previously described (*7*). Libraries were then purified using KAPA Pure Beads (Roche). Paired-end sequencing of enriched libraries was performed on a NextSeq 500 Sequencer (Illumina, San Diego, CA, USA) using the NextSeq 500/550 Mid Output Kit v2.5 (300 cycles) (Illumina).

The HVR was amplified using a OneStep RT-PCR Kit (Qiagen) with specific primers, ratHVR-s (5′ – CAY CTC CCW GGC GAY GAG ATG TA – 3′) and ratHVR-as (5′ – TGC AGY CCR ACR TGY GGG GTC AT – 3′), based on aligned ratHEV C1 sequences. Each reaction contained 0.4 mM dNTPs, 5 µl Q-solution, 0.25 U/µl RNase inhibitor (Qiagen), 0.8 µM of each primer, and 2.5 µl nucleic acid, with the following cycling conditions: 50°C for 60 min, 95°C for 15 min, 40 cycles of 95°C for 30 s, 56°C for 30 s and 72°C for 35 s, and a final elongation of 72°C for 5 min. The product was size separated by gel electrophoresis, purified, and sequenced by Sanger dideoxy chain-termination sequencing (Eurofins Genomics, Ebersberg, Germany). HTS data were analyzed in Geneious Prime® 2020.2.2 (Biomatters Ltd Auckland, New Zealand), and set paired reads were trimmed using the BBDuk Plug-in. Reads were then

mapped to reference sequences (GenBank accession numbers: GU345042, MW795567, and KM516906). The almost complete genome sequences were uploaded to GenBank with accession numbers PZ581217- PZ581222.

Immunohistochemistry

Paraffin-embedded tissue sections were prepared following standard protocols. Briefly, tissues were fixed in 4% paraformaldehyde (PFA), trimmed, and embedded in paraffin. Sections of 3 µm thickness were cut, mounted on SuperFrost® Plus slides (Carl Roth GmbH, Karlsruhe, Germany), and subsequently deparaffinized.

Endogenous peroxidase activity was blocked by incubation in 3% hydrogen peroxide (H_2O_2) (Merck, Darmstadt, Germany). Slides were rinsed in distilled water and subjected to heat-induced antigen retrieval in citrate buffer (pH 6.0) for 20 min at 100°C using a steamer (Sichler, NX-3213–675, Buggingen, Germany). After cooling to room temperature, sections were transferred to cover plates (Themo Fisher Scientific, Waltham, MA, USA) and washed three times in Tris-buffered saline (TBS).

Non-specific binding was blocked by incubation with goat serum for 30 min at room temperature. Sections were then incubated for 1 h at room temperature with a primary antiserum against Dobrava-Belgrade virus (DOBV) nucleocapsid protein (in-house, swine-derived; 1:1000 dilution), selected based on its known cross-reactivity with related hantaviruses (*8*).

Following three washes in TBS, sections were incubated with a biotinylated goat anti-swine secondary antibody (1:200 dilution; Jackson ImmunoReserarch, West Grove, PA, USA; 114–066–003) for 20 min at room temperature. After additional washes (3× TBS), slides were incubated with avidin-biotin complex (ABC) reagent (Vectastain Elite, PK 6100, Vector Laboratories, Newark, CA, USA) for 30 min, followed by three further TBS washes.

Visualization was performed using 3-amino-9-ethylcarbazole (AEC) substrate (abcam, ab64252, Cambridge, UK) for 10 min. Slides were washed with deionized water, counterstained with hematoxylin, and rinsed in cold running tap water for 10 min to allow bluing. This was followed by a 5 min wash in distilled water. Finally, sections were mounted using Aquatex mounting medium (Merck).

RNA in situ hybridization

In situ hybridization (ISH) was performed on 4 µm thick formalin-fixed, paraffin-embedded (FFPE) tissue sections mounted on adhesive microscope slides (Starfrost®, Engelbrecht Medizin- & Labortechnik GmbH, Edermünde, Germany) with RNAscope (Advanced Cell Diagnostics, Inc., Newark, CA, USA) using the 2.5. HD Assay-RED, following the manufacturer's protocol with minor changes. Deparaffinization using xylene was repeated three times. The Isotemp Hybridization Incubator (CAT. 13–247–20, Fisher Scientific, Schwerte, Germany) was used as the hybridization oven and all wash steps were performed in a 200 ml Coplin jar. Standard conditions were used for target retrieval (15 min) and Protease Plus treatment (30 min). FFPE blocks from eight rats were provided in a blinded fashion. Based on the full genome sequence from rat KS22/001, a 20ZZ RNA probe, targeting the ORF1 sequence (nucleotides, nt, 2930–4312), was designed by Advanced Cell Diagnostics (Cat. No. 1333041-C1). A commercial 3-plex DapB probe (cat. no. 320871) was used as a negative control. A representative hematoxylin and eosin-stained liver section is shown as morphologic overview in Appendix Figure 2A.

Multiplex serology

The multiplex HEV serology was based on an immunosorbent assay in combination with the fluorescent bead technology from Luminex Corporation (Luminex Corp., Austin, TX, USA) and comprises ratHEV, genotype HEV-3, and an immunoglobulin (Ig) G control. General set-up and protocol of the multiplex serology is described elsewhere, with slight modifications (*9–11*).

The truncated ratHEV and HEV-3 capsid protein antigens were produced as N terminally His-tagged fusion proteins in *Escherichia coli,* as previously described (*12*,*13*). The purified antigens were subsequently dialyzed against phosphate-buffered saline (PBS), lyophilized, reconstituted in distilled water, and coupled to polystyrene beads with distinct embedded fluorescent dyes (MagPlex® Microspheres). For the IgG control, an additional bead set was coated with anti-rat IgG (AffiniPure donkey anti-rat IgG (H + L), 4 µg/ml beads; cat. no. 712–005–150, Jackson ImmunoResearch Laboratories, Inc., West Grove, PA, USA). Sera and transudates were diluted 1:250 and 1:50, respectively, in pre-incubation buffer (1 g/l casein, 5 g/l polyvinyl alcohol, 8 g/l polyvinylpyrrolidone, 2 g/l total protein lysate from bacteria overexpressing glutathione S-transferase tag without adhering sequences to block binding of antibodies in 1× PBS) and incubated for 1 h at room temperature to suppress unspecific binding

of antibodies to the beads themselves. The differently labeled recombinant viral antigen or anti-IgG loaded beads were mixed to be incubated with an equal volume of diluted serum/transudate in a single reaction on a 96-well plate (final dilution 1:500 for rat sera and 1:100 for rat transudates).

The Luminex analyzer BioPlex200 (BioRad Laboratories GmbH, Munich, Germany) was used to distinguish between the bead set, and consequently the bound viral antigen, and to quantify the amount of bound serum antibody by a secondary antibody (biotinylated AffiniPure goat anti-rat IgM + IgG [H+L; cat. no. 112–065–068; Jackson ImmunoResearch Laboratories], 1:1000 diluted in blocking buffer [1 g/l casein in 1× PBS]) and a fluorescent reporter conjugate (Streptavidin-R-Phycoerythrin, MOSS Inc., Pasadena, CA, USA; 1:500 diluted in blocking buffer). To assess background reactivity, all bead sets were additionally run in parallel without serum. Final mean fluorescence intensity (MFI) values were measured of at least 50 beads per bead set and sample; background reactivity was accounted for by subtracting the individual bead MFI values resulting from a serum-free reaction. The cutoff was calculated as the mean MFI value of the negative sample set (n = 77) plus three times the standard deviation. Samples were considered positive if the calculated cutoff exceeded 400 MFI for HEV-3 or 120 MFI for ratHEV.

Western blot analysis of rat blood samples

Sera and transudates were diluted 1:500 and 1:30, respectively, in PBS containing 0.1% Tween 20 (PBS-T) and analyzed by Western blot using truncated ratHEV and HEV-3 capsid antigens. Recombinant maltose binding protein (MBP) expressed in *Escherichia coli* was included as a negative control antigen. Proteins were separated by SDS-PAGE in 12% polyacrylamide gels and transferred onto PVDF membranes (GE Healthcare Life Science, Freiburg, Germany) under semidry conditions. Membranes were blocked with 1× Roti-Block solution (Carl Roth GmbH, Karlsruhe, Germany) for 1 h at room temperature with shaking and incubated overnight with the diluted rat samples. After washing with PBS-T, membranes were incubated for 2 h at room temperature with horse radish peroxidase (HRP)-conjugated anti-rat IgG Fc antibody (1:1000 dilution in TBS-T; Invitrogen, USA). Following additional washes with PBS-T, bound antibodies were visualized using 4-chloro-1-naphthol (Sigma-Aldrich, St. Louis, MO, USA) and hydrogen peroxide. Sera of rats immunized with purified *E. coli*-expressed truncated ratHEV and HEV-3 capsid antigens were used as positive control sera (*12–14*).

These two truncated capsid protein antigens of ratHEV and HEV-3 were previously successfully used to differentiate between ratHEV and HEV-3 reactive antibodies in rats and humans, using an IgG ELISA (*12–14*).

Phylogenetic reconstruction

The best-fit nucleotide substitution model, determined using JModelTest2 (*15*), was the generalized time reversible model (GTR). Phylogenetic trees were generated in MrBayes v.3.2.7 (*16*) using short ORF1 sequences (276 nt) and full genome sequences from the start of ORF1 to the end of ORF2, 20 million generations sampled every 2000, with the first 25% discarded as burn-in.

References

1. Ryll R, Bernstein S, Heuser E, Schlegel M, Dremsek P, Zumpe M, et al. Detection of rat hepatitis E virus in wild Norway rats (*Rattus norvegicus*) and Black rats (*Rattus rattus*) from 11 European countries. Vet Microbiol. 2017;208:58–68. PubMed https://doi.org/10.1016/j.vetmic.2017.07.001

2. Johne R, Plenge-Bönig A, Hess M, Ulrich RG, Reetz J, Schielke A. Detection of a novel hepatitis E-like virus in faeces of wild rats using a nested broad-spectrum RT-PCR. J Gen Virol. 2010;91:750–8. PubMed https://doi.org/10.1099/vir.0.016584-0

3. Baylis SA, Adlhoch C, Childs L, Stühler A, Karlsson M, Molier M, et al.; HEV Sequencing Study Group. An evaluation of hepatitis E virus molecular typing methods. Clin Chem. 2021;68:181–91. PubMed https://doi.org/10.1093/clinchem/hvab186

4. Caballero-Gómez J, Casares-Jiménez M, Gallo-Marín M, Pereira-Pardo S, Beato-Benítez A, Poyato A, et al.; GEHEP-014 Study Group. Rat hepatitis E virus as an aetiological agent of acute hepatitis of unknown origin. J Hepatol. 2025;83:662–9. PubMed https://doi.org/10.1016/j.jhep.2025.02.027

5. Sridhar S, Yip CCY, Wu S, Cai J, Zhang AJ-X, Leung K-H, et al. Rat hepatitis E virus as cause of persistent hepatitis after liver transplant. Emerg Infect Dis. 2018;24:2241–50. PubMed https://doi.org/10.3201/eid2412.180937

6. de Cock MP, de Vries A, Fonville M, Esser HJ, Mehl C, Ulrich RG, et al. Increased rat-borne zoonotic disease hazard in greener urban areas. Sci Total Environ. 2023;896:165069. PubMed https://doi.org/10.1016/j.scitotenv.2023.165069

7. Schilling-Loeffler K, Viera-Segura O, Corman VM, Schneider J, Gadicherla AK, Schotte U, et al. Cell culture isolation and whole genome characterization of hepatitis E virus strains from wild boars in Germany. Microorganisms. 2021;9:2302. PubMed https://doi.org/10.3390/microorganisms9112302

8. Raftery MJ, Lalwani P, Lütteke N, Kobak L, Giese T, Ulrich RG, et al. Replication in the mononuclear phagocyte system (MPS) as a determinant of hantavirus pathogenicity. Front Cell Infect Microbiol. 2020;10:281. PubMed https://doi.org/10.3389/fcimb.2020.00281

9. Waterboer T, Sehr P, Michael KM, Franceschi S, Nieland JD, Joos TO, et al. Multiplex human papillomavirus serology based on in situ-purified glutathione s-transferase fusion proteins. Clin Chem. 2005;51:1845–53. PubMed https://doi.org/10.1373/clinchem.2005.052381

10. Waterboer T, Sehr P, Pawlita M. Suppression of non-specific binding in serological Luminex assays. J Immunol Methods. 2006;309:200–4. PubMed https://doi.org/10.1016/j.jim.2005.11.008

11. Schmidt K, Butt J, Mauter P, Vogel K, Erles-Kemna A, Pawlita M, et al. Development of a multiplex serological assay reveals a worldwide distribution of murine astrovirus infections in laboratory mice. PLoS One. 2017;12:e0187174. PubMed https://doi.org/10.1371/journal.pone.0187174

12. Dremsek P, Wenzel JJ, Johne R, Ziller M, Hofmann J, Groschup MH, et al. Seroprevalence study in forestry workers from eastern Germany using novel genotype 3- and rat hepatitis E virus-specific immunoglobulin G ELISAs. Med Microbiol Immunol. 2012;201:189–200. PubMed https://doi.org/10.1007/s00430-011-0221-2

13. Johne R, Dremsek P, Kindler E, Schielke A, Plenge-Bönig A, Gregersen H, et al. Rat hepatitis E virus: geographical clustering within Germany and serological detection in wild Norway rats (*Rattus norvegicus*). Infect Genet Evol. 2012;12:947–56. PubMed https://doi.org/10.1016/j.meegid.2012.02.021

14. Kubickova B, Schenk JA, Ramm F, Markuškienė K, Reetz J, Dremsek P, et al. A broadly cross-reactive monoclonal antibody against hepatitis E virus capsid antigen. Appl Microbiol Biotechnol. 2021;105:4957–73. PubMed https://doi.org/10.1007/s00253-021-11342-7

15. Darriba D, Taboada GL, Doallo R, Posada D. jModelTest 2: more models, new heuristics and parallel computing. Nat Methods. 2012;9:772. PubMed https://doi.org/10.1038/nmeth.2109

16. Ronquist F, Teslenko M, van der Mark P, Ayres DL, Darling A, Höhna S, et al. MrBayes 3.2: efficient Bayesian phylogenetic inference and model choice across a large model space. Syst Biol. 2012;61:539–42. PubMed https://doi.org/10.1093/sysbio/sys029

17. Heuser E, Drewes S, Trimpert J, Kunec D, Mehl C, de Cock MP, et al. Pet rats as the likely reservoir for human Seoul Orthohantavirus infection. Viruses. 2023;15:467. PubMed https://doi.org/10.3390/v15020467

18. Hofmann J, Ulrich RG, Mehl C, Drewes S, Esser J, Loyen M, et al. Hantavirus disease cluster caused by Seoul virus, Germany. Emerg Infect Dis. 2024;30:133–5. PubMed https://doi.org/10.3201/eid3001.230855

Appendix Table 1. Results of molecular and serologic pet rat hepevirus screening, ratHEV in situ hybridization, and SEOV IHC analyses*

Instances of detection	Animal ID	Year	Sex	RT-qPCR SEOV (liver)	NBS RT-PCR (sequencing result)	RT-qPCR ratHEV (liver)	Multiplex serology		WB		ISH ratHEV (liver)	ratHEV accession number	IHC SEOV (liver)
							HEV-3	ratHEV	HEV-3	ratHEV			
1	KS19/1352†	2019	M	**Pos** (*17*)	Neg	Neg	Neg	**Pos**	Neg	**Pos**	Neg	n.a.	**Pos**
	KS19/1353†		M	**Pos** (*17*)	Neg	Neg	Neg	**Pos**	**Pos**	**Pos**	Neg	n.a.	Neg
	KS19/1354†		M	**Pos** (*17*)	**Pos (ratHEV)**	**Pos**	Neg	**Pos**	Neg	**Neg**	**Pos**	PZ581218	**Pos**
	KS19/1414†		F	Neg (*17*)	Neg	Neg	Neg	**Neg**	NT	NT	NT	n.a.	NT
	KS19/2195‡		M	**Pos** (*17*)	Neg	Neg	Neg	**Pos**	**Pos**	**Pos**	Neg	n.a.	Neg
	KS19/2196‡		M	**Pos** (*17*)	**Pos (ratHEV)**	**Pos**	**Pos**	**Pos**	**Pos**	**Pos**	**Pos**	PZ581219	Neg
	KS19/2197‡		M	Neg (*17*)	Neg	Neg	Neg	**Pos**	**Pos**	**Pos**	Neg	n.a.	Neg
2	KS21/4038	2021	F	**Pos** (*18*)	Neg	Neg	**Pos**	**Pos**	**Pos**	**Pos**	NT	n.a.	Neg
	KS21/4039		F	**Pos** (*18*)	Neg	Neg	Neg	**Pos**	**Pos**	**Pos**	NT	n.a.	Neg
	KS21/4040		F	**Pos** (*18*)	Neg	Neg	**Pos**	**Pos**	**Pos**	**Pos**	NT	n.a.	**Pos**
	KS21/4041		F	**Pos** (*18*)	Neg	Neg	Neg	**Pos**	**Pos**	**Pos**	NT	n.a.	**Pos**
3	KS22/001	2021	M	**Pos** (*18*)	**Pos (ratHEV)**	**Pos**	Neg	**Pos**	**Pos**	**Pos**	**Pos**	PZ581217	Neg
	KS22/002		M	**Pos** (*18*)§	Neg	NA	Neg	**Pos**	**Pos**	**Pos**	NA	n.a.	NA

*Representative liver sections are shown with ISH for ratHEV RNA detection and with IHC for SEOV antigen detection in Appendix Figure 2. IHC, immunohistochemistry; ISH, in situ hybridization; n.a., not applicable; NA, tissue not available; NBS, nested broad spectrum; NT, not tested; ratHEV, rat hepatitis E virus; RT-PCR, reverse transcription PCR; RT-qPCR, real-time reverse transcription PCR; SEOV, Seoul virus; WB, Western blot assay.
†Pet rats from pet rat owner 1 (patient).
‡Pet rats from pet rat owner 2.
§Liver tissue was unavailable, so RNA was detected based on heart and lung.

Appendix Table 2. Nucleotide (nt) and amino acid (aa) sequence similarity of the three pet rat-derived ratHEV sequences. Full genome sequence comparison includes full coding regions and non-coding regions flanking ORFs*.

Sequence region		% identity
Full genome sequence	nt	99.70–99.86
ORF1	nt	99.65–99.83
	aa	99.20–99.76
ORF2	nt	99.87–99.97
	aa	99.69–99.84
ORF3	nt	99.72–100
	aa	99.15–100
ORF4	nt	99.91–100
	aa	99.45–100

*ORF, open reading frame.

Appendix Table 3. Nucleotide (nt) and amino acid (aa) sequence similarity (in %) of pet rat-derived ratHEV sequences compared to wild rat-derived ratHEV sequences from Rotterdam, the Netherlands (NLD) and Hamburg, Germany (DE) and a human-derived ratHEV sequence from Berlin, DE. Full genome sequence comparison includes full coding regions and non-coding regions flanking ORFs*.

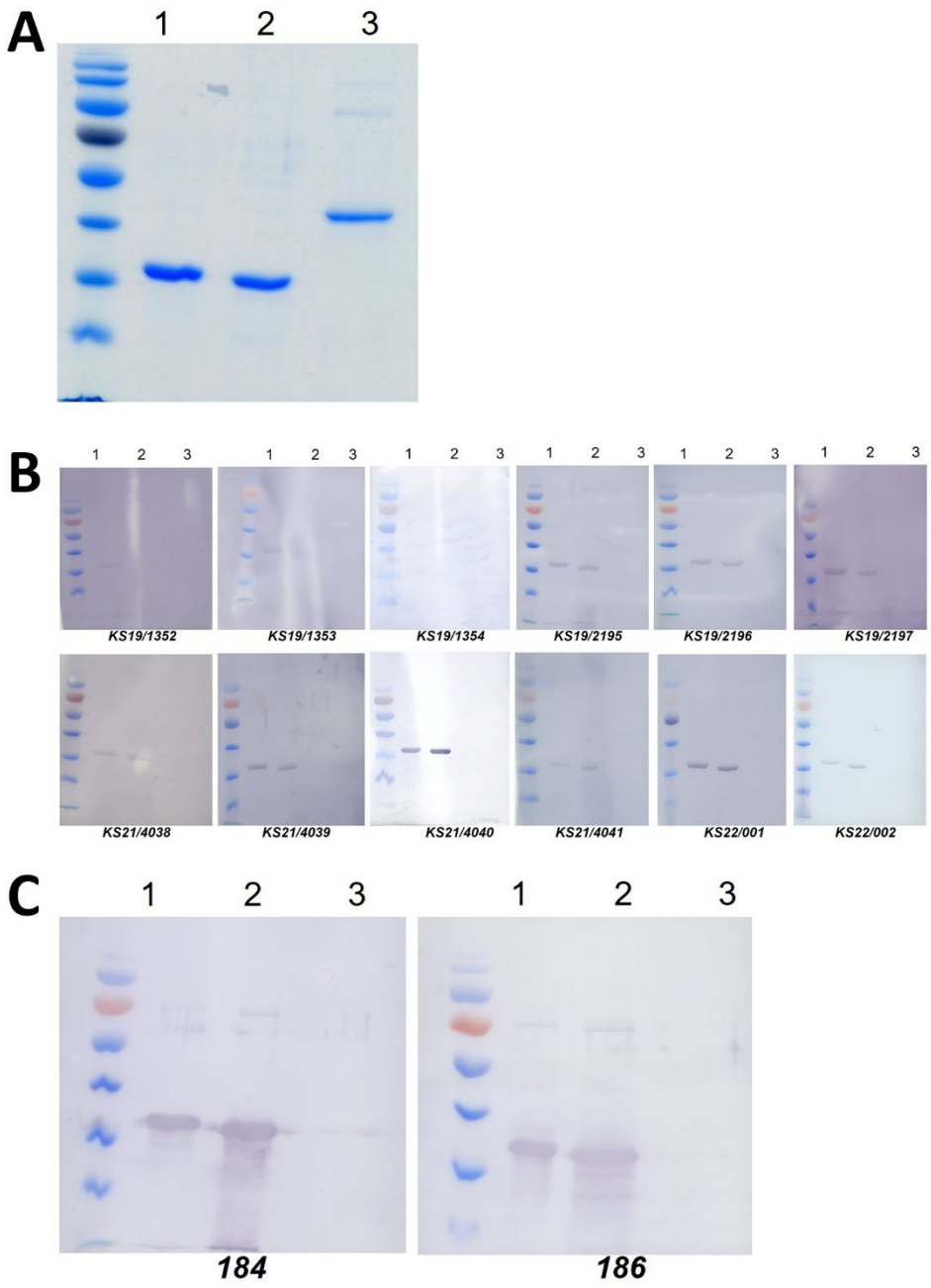
		Wild rat–derived sequences					Human-derived sequence
Sequence region		M226 NLD, Rotterdam	M186 NLD, Rotterdam	M268 NLD, Rotterdam	GU345042 DE, Hamburg	GU345043 DE, Hamburg	PV252688 DE, Berlin
Full genome	nt	99.24–99.39	92.25–92.30	87.25–87.33	89.18–89.27	89.27–89.32	86.81–86.83
ORF1	nt	99.23–99.38	91.77–91.86	86.33–86.39	88.37–88.42	88.34–88.40	85.77–85.87
	aa	99.08–99.82	96.88–97.37	93.82–94.37	95.60–96.09	95.23–95.72	94.55–95.04
ORF2	nt	99.41–99.53	93.44–93.46	89.61–89.74	91.68–91.81	91.96–92.02	89.43–89.56
	aa	99.69–99.84	98.76–98.91	97.83–97.98	97.05–97.20	97.98–97.14	97.98–98.14
ORF3	nt	99.44–99.72	94.4–94.68	89.64–89.92	91.60–91.88	92.44–92.72	89.78–90.06
	aa	98.31–99.15	88.14–88.98	75.42–75.42	82.20–82.20	83.90–83.90	77.12–77.12
ORF4	nt	99.73–99.82	97.92–98.01	94.47–94.57	94.66–94.75	94.11–94.2	94.66–94.75
	aa	99.45–100	95.63–96.17	85.79–86.34	86.34–86.89	85.79–86.34	86.34–86.89

*aa, amino acid; DE, Germany; nt, nucleotide; ORF, open reading frame.

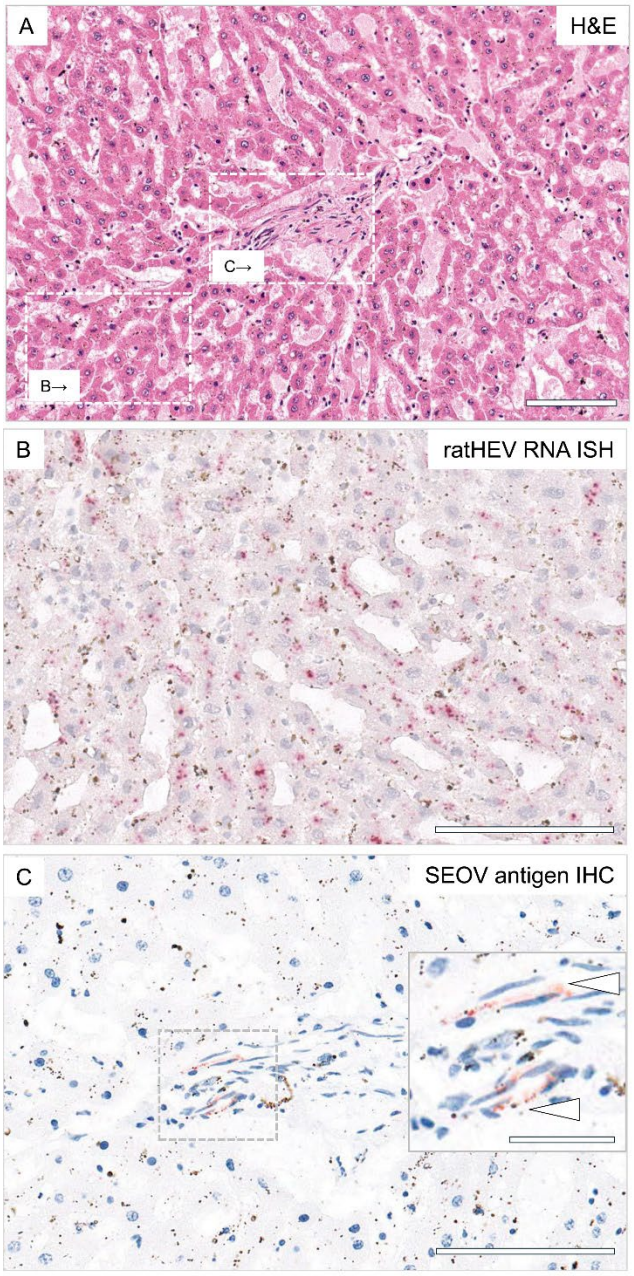
Appendix Table 4. Results of SEOV IHC and ratHEV ISH. A representative hematoxylin and eosin-stained liver section is shown as morphologic overview in Appendix Figure 2A, including ISH for ratHEV detection (Appendix Figure 2B), and IHC for SEOV detection (Appendix Figure 2C)*

			Tissue															
Instances of			Liver		Lung		Kidney		Heart		Spleen		Brain		Intestine		Testes/Ovaries	
detection	Animal ID	Year	rHEV ISH	SEOV IHC	rHEV ISH	SEOV IHC	rHEV ISH	SEOV IHC	rHEV ISH	SEOV IHC	rHEV ISH	SEOV IHC	rHEV ISH	SEOV IHC	rHEV ISH	SEOV IHC	rHEV ISH	SEOV IHC
1	KS19/1352†	2019	Neg	**Pos**	NT	**Pos**	NT	**Pos**	NT	Neg	NT	**Pos**	NT	**Pos**	NT	**Pos**	NT	Neg
	KS19/1353†		Neg	Neg	NT	**Pos**	NT	**Pos**	NT	Neg	NT	**Pos**	NT	Neg	NT	Neg	NT	Neg
	KS19/1354†		**Pos**	**Pos**	NT	**Pos**	NT	**Pos**	NT	Neg	NT	**Pos**	NT	**Pos**	**Pos** (intestinal lumen)	**Pos**	NT	Neg
	KS19/1414†		NT	NT	NT	NT	NT	NT	NT	NT	NT	NT	NT	NT	NT	NT	NT	NT
	KS19/2195‡		Neg	Neg	NT	**Pos**	NT	**Pos**	NT	Neg	NT	NT	NT	**Pos**	NT	**Pos**	NT	Neg
	KS19/2196‡		**Pos**	Neg	Neg	Neg	NT	**Pos**	NT	Neg	NT	Neg	NT	Neg	NT	Neg	NT	Neg
	KS19/2197‡		Neg	Neg	NT	Neg	NT	Neg	NT	Neg	NT	Neg	NT	Neg	NT	Neg	NT	Neg
2	KS21/4038	2021	NT	Neg	NT	Neg	NT	**Pos**	NT	Neg	NT	Neg	NT	Neg	NT	Neg	NT	NT
	KS21/4039		NT	Neg	NT	Neg	NT	Neg	NT	Neg	NT	NT	NT	Neg	NT	Neg	NT	NT
	KS21/4040		NT	**Pos**	NT	Neg	NT	**Pos**	NT	Neg	NT	**Pos**	NT	**Pos**	NT	**Pos**	NT	NT
	KS21/4041		NT	**Pos**	NT	Neg	NT	Neg	NT	**Pos**	NT	**Pos**	NT	**Pos**	NT	**Pos**	NT	NT
3	KS22/001	2021	**Pos**	Neg	NT	Neg	Neg	**Pos**	NT	Neg	**Pos**	NT	NT	**Pos**	NT	NT	NT	NT
	KS22/002		NT	NT	NT	Neg	NT	NT	NT	Neg	NT	NT	NT	Neg	NT	NT	NT	NT

*IHC, immunohistochemistry; ISH, in situ hybridization; n.a., not applicable; NA, tissue not available; NT, tissue not tested; rHEV, rat hepatitis E virus; SEOV, Seoul virus.
†Pet rats from pet rat owner 1 (patient).
‡Pet rats from pet rat owner 2.



Appendix Figure 1. Western blot analysis of rat blood samples. (A) SDS-PAGE of recombinant antigens used for western blotting. (B) Western blot analysis of pet rat blood samples. (C) Western blot analysis of control rat blood serum samples: serum sample of a rat immunized with truncated HEV-3 capsid protein (184) and of a rat immunized with truncated ratHEV capsid protein (186). Lane 1, truncated ratHEV capsid protein; lane 2, truncated HEV-3 capsid protein; lane 3, maltose binding protein (MBP) used as negative control antigen. All proteins were expressed in *Escherichia coli*. Sample IDs are shown below each blot.



Appendix Figure 2. Histological detection of rat hepatitis E virus RNA and Seoul virus antigen in liver tissue from rat KS19/1354. (A) Hematoxylin and eosin (H&E)-stained liver section shown as a morphological overview. Dashed boxes indicate representative regions comparable to those analyzed in panels B and C. (B) Detection of rat hepatitis E virus (ratHEV) RNA by in situ hybridization (ISH), visible as punctate red hybridization signals within hepatocytes. (C) Detection of Seoul virus (SEOV) antigen by immunohistochemistry (IHC), showing red chromogenic staining in endothelial cells. The inset shows a higher magnification view of the boxed area in panel C; arrowheads indicate representative SEOV antigen-positive cells. Nuclei are counterstained blue with hematoxylin in panels B and C. Scale bars: 100 μm in A–C; 25 μm in the inset.